6. Yu. A. Buevich, "Movement of bubbles in a fluidized bed," Izv. Akad. Nauk SSSR, Mekh. Zhidk. Gaza, No. 3, 43-51 (1975).
7. Yu. P. Gupalo, Yu. S. Ryazantsev, and Yu. A. Sergeev, "Bubble growth in a fluidized bed with nonlinear phase interaction," Izv. Akad. Nauk SSSR, Mekh. Zhidk. Gaza, No. 6, 66-73 (1977).
8. Yu. A. Buevich and I. M. Tsyrul'nikov, "Evolution of the inhomogeneous state in a fluidized bed," Inzh.-Fiz. Zh., 40, No. 4, 696-704 (1981).
9. J. F. Davidson and D. Harrison (eds.), Fluidization, Academic Press (1971).
10. V. D. Goroshko, R. B. Rozenbaum, and O. M. Todes, "Approximate laws of hydraulics of a fluidized bed and constrained fall," Izv. Vyssh. Uchebn. Zaved., Neft' Gaz, No. 1, 125-131 (1958).
11. D. Kunin and O. Levenshpil', Commercial Fluidization [Russian translation], Khimiya, Moscow (1976).
12. D. Geldart, "The expansion of a bubbling fluidized bed," Powder Technol., 1, No. 6, 355-368 (1968).
13. M. P. Subwari, R. Clift, and D. L. Pyle, "Bubbling behavior of fluidized beds at elevated pressures," Fluidization — Proceedings of the 2nd Eng. Found. Conf., Cambridge, England, Cambridge Univ. Press (1978), pp. 50-54.
14. T. Varadi and J. R. Grace, "High pressure fluidization in a two-dimensional bed," Fluidization — Proceedings of the 2nd Eng. Found. Conf., Cambridge, England, Cambridge Univ. Press (1978), pp. 55-58.
15. V. A. Borodulya, Yu. A. Buevich, and V. I. Dikalenko, "Study of the motion and mass transfer of bubbles in a fluidized bed," Inzh.-Fiz. Zh., 41, No. 4, 678-689 (1981).
16. A. A. Oigenblik, A. S. Zheleznov, and M. G. Slin'ko, "Study of longitudinal mixing and phase exchange in a free fluidized bed," Dokl. Akad. Nauk SSSR, 222, No. 4, 901-903 (1975).

PACKET MODEL OF EXTERNAL HEAT TRANSFER FOR A FLUIDIZED BED

V. A. Borodulya and V. I. Kovenskii

UDC 66.096.5

A modification is proposed for the packet model of external heat transfer of a fluidized bed. The modified model considers heat exchange between the particles and the gas flowing through the packet formed by the particles.

As is known, a fluidized bed is characterized by a discrete structure [1]. The effect of this structure on external heat transfer is evidently best accounted for by the packed model described in detail in [1-3]. According to this model, rising gas bubbles mix with dispersed material and continuously move packets of particles from the core of the bed to the wall of the heat exchanger. Approaching the wall, the packets, in the process of nonsteady heat conduction, give up the heat they accumulated in the core (henceforth, it is assumed that the temperature of the heat exchanger is lower than the temperature of the bed). The packet model most accurately describes heat exchange in a fluidized bed of fine ($d_p \leq 0.5$ mm) particles [3].

Another well-known mechanism — convective heat transfer by a filtering gas — determines heat transfer in a bed of coarse ($d_p > 5$ mm) particles [3].

In accordance with the assumption of the additivity of the components of external heat transfer [1-6], transport models corresponding to the limiting cases of fine and coarse particles are used jointly to describe the process in a fairly broad and practicable range of intermediate dispersed-material sizes ($0.5 < d_p < 5$ mm). Here, an increase in particle size changes the relative contribution of the main heat-transfer mechanisms.

A. V. Lykov Institute of Heat and Mass Transfer, Academy of Sciences of the Belorussian SSR, Minsk. Translated from Inzhnerno-Fizicheskii Zhurnal, Vol. 47, No. 5, pp. 789-796, November, 1984. Original article submitted November 4, 1983.

 0022-0841/84/4705-1322$08.50

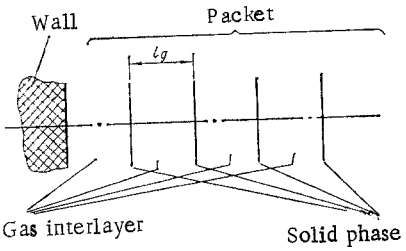

Fig. 1. Model for calculating nonsteady heat exchange between packet and surface.

Convective heat transfer intensifies with an increase in d_p, since there is a rapid increase in gas filtration velocity [3, 4]. Within the framework of the existing model, the reduction in the contribution of the packet mechanism in the transition to coarse particles is due to the thermal inertia of the particles, which do not have the time to cool while the packet is near the wall [6]. However, this explanation contradicts the results of experiments involving the cooling of particles close to a heat-exchanger surface in a high-temperature bed [5]. This contradiction is evidence of the approximate nature of the model.

In our opinion, the packet model can be improved if we consider that the gas continuously blows through the packet and is capable by means of phase exchange of transferring heat to the particles from the core of the bed and thus compensating for the thermal losses of the particles during cooling at the wall. The exact number of particles receiving heat from the gas and the temperature distribution in the filtering flow are indeterminate and change randomly. Thus, in this article we assume that the mean temperature of the gas in a packet is always equal to the temperature in the core of the bed and that the heat received by the solid phase can be calculated using the effective phase-heat-exchange coefficient, found by the formulas [3]

$$\mathrm{Nu}^* = 0.016\,\mathrm{Pr}^{1/3}\left(\frac{\mathrm{Re}}{\varepsilon}\right)^{1.3},\quad 0.1 < \frac{\mathrm{Re}}{\varepsilon} < 200, \tag{1a}$$

$$\mathrm{Nu}^* = 0.4\,\mathrm{Pr}^{1/3}\left(\frac{\mathrm{Re}}{\varepsilon}\right)^{2/3},\quad 200 < \frac{\mathrm{Re}}{\varepsilon} < 10^5. \tag{1b}$$

Here, it is considered that the porosity of the packet and the velocity of the filtering gas are connected by the relation [2] $\varepsilon = ((18\mathrm{Re} + 0.36\mathrm{Re}^2)/\mathrm{Ar})^{0.21}$, just as for a homogeneous bed.

The model proposed in [6] is used to calculate nonsteady heat exchange between the packet and the surface. In this model, rows of particles in the packet are replaced by thermally infinite thin strips with a heat capacity $(1-\varepsilon)y_p d_p C_p \rho_p S$ (S is the area of any element of the model) and separated by layers of the medium of thickness $l_g = \varepsilon y_p d_p$ with a thermal conductivity λ_e (Fig. 1). The thickness of the intervening gas layer between the wall and the first row of particles, not determinable unambiguously, was taken equal to l_g. With this choice, the following condition [7] is satisfied:

$$\lim_{\tau \to 0} \mathrm{Nu}_e = 2, \tag{2}$$

The effective thermal conductivity was calculated from Bruggman's formula [8]. Given the condition $\lambda_p/\lambda_g > 20$, this formula is usually valid for a gas fluidized bed and takes the form

$$\lambda_e = \frac{\lambda_g}{\varepsilon^{1.5}}. \tag{3}$$

During cooling at the wall of the heat exchanger, the heat content of any of N rows of particles changes as a result of heat conduction between adjacent rows (the heat flux between the i-th and i + 1-st rows $q = -\lambda_e(t_{i+1}^N - t_i^N)/l_g$) and as a result of heat exchange with the filtering gas (the heat flux to the i-th row of particles is $6(1-\varepsilon)y_p\alpha^*(t_b - t_i^N)$). This process is described by the following system of ordinary differential equations in the dimensionless temperatures of N rows of particles forming packets (a detailed description of the derivation of the system is given in [6], which, in contrast to this

article, introduces contact resistance and does not consider heat exchange between the particles and gas):

$$\dot{\vartheta}_i^N = c_1(\vartheta_{i+1}^N - 2\vartheta_i^N + \vartheta_{i-1}^N) + c_2(1 - \vartheta_i^N) \tag{4}$$

with the initial conditions $\vartheta_i^N|_{\tau=0} = 1$, $i = 1, \ldots, N$, where

$$c_1 = \frac{\lambda_e}{C_p\rho_p\varepsilon(1-\varepsilon)y_p^2 d_p^2}; \quad c_2 = \frac{6\alpha^*}{C_p\rho_p d_p};$$

$$\vartheta_i^N = \frac{t_i^N - t_w}{t_b - t_w}.$$

System (4), with an arbitrary N, is solved numerically. An analytical solution can be written for two special cases N = 1 and N → ∞.

When N = 1,

$$\vartheta_1^1(\tau) = \frac{Y}{1+2Y}\exp\left(-\frac{\tau}{K\tau_0}\right) + \bar{\vartheta}_1^1,$$

where

$$\bar{\vartheta}_1^1 = \frac{1+Y}{1+2Y}; \quad K = \frac{2Y}{1+2Y}; \quad \tau_0 = \frac{1}{2c_1};$$

$$Y = \frac{\lambda_e}{6(1-\varepsilon)\varepsilon y_p^2 \lambda_g \mathrm{Nu}^*}; \tag{5}$$

K is a dimensionless parameter determining the change in the time constant of a single-row packet in relation to the ratio of the conductive heat flow from the particles to the surface to the heat transfer from the filtering gas to the particles; Y is a dimensionless parameter equal to this ratio.

When N → ∞,

$$\vartheta_i^\infty(\tau) = 1 - \frac{1}{2}\left[\exp\left(\frac{i}{\sqrt{Y}}\right)\operatorname{erfc}\left(\frac{i}{2\sqrt{c_1\tau}} + \sqrt{c_2\tau}\right) + \exp\left(-\frac{i}{\sqrt{Y}}\right)\operatorname{erfc}\left(\frac{i}{2\sqrt{c_1\tau}} - \sqrt{c_2\tau}\right)\right],$$

$$\bar{\vartheta}_i^\infty = 1 - \exp\left(-\frac{i}{\sqrt{Y}}\right), \quad i = 1, \ldots, \infty. \tag{6}$$

It can be seen from Eqs. (5) and (6) that the dimensionless parameter Y completely determines the solution of system (4) for a single-row packet and to a large degree determines the solution for a infinite packet. In connection with this, it is best to explain how this parameter changes and, thus, how Eqs. (5) and (6) change in relation to the diameter of the fluidized particles.

The following limit relations can be written for very small values of d_p:

$$\mathrm{Nu}^* \to 0, \quad Y \to \infty,$$

here K → 1,

$$\vartheta_1^1(\tau) \to \frac{1}{2}\left[\exp\left(-\frac{\tau}{\tau_0}\right) + 1\right], \quad \vartheta_i^\infty(\tau) \to 1 - \operatorname{erfc}\left(\frac{i}{2\sqrt{c_1\tau}}\right), \quad \bar{\vartheta}_i^\infty \to 0. \tag{7}$$

It can be seen from Eqs. (7) that for very small particles Eqs. (5) and (6) coincide at the limit with the solution of the problem of nonsteady cooling of a packet through which no gas flows [6].

As particle diameter increases, there is a rapid increase in phase heat exchange. At the limit we can write

$$\mathrm{Nu}^* \to \infty, \quad Y \to 0, \quad K \to 0, \quad \vartheta_1^1(\tau) \to 1, \quad \bar{\vartheta}_1^1 \to 1, \quad \vartheta_i^\infty(\tau) \to 1, \quad \bar{\vartheta}_i^\infty \to 1. \tag{8}$$

It follows from limit relations (8) that the rate of phase heat exchange in a packet of very coarse particles is high enough to compensate for the heat lost by the particles as a result of heat conduction to the wall. Here, the temperature of the solid phase remains

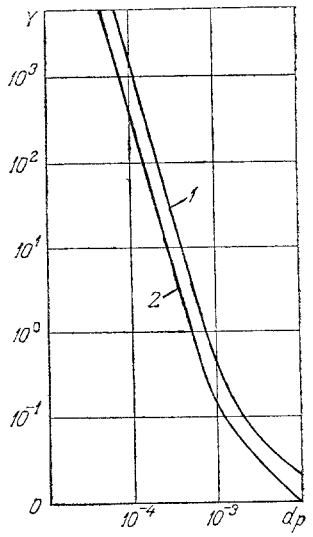

Fig. 2

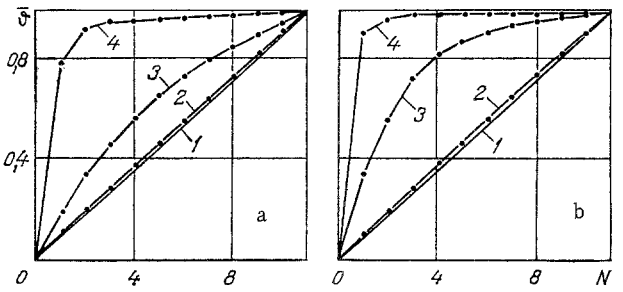

Fig. 3

Fig. 2. Dependence of the dimensionless parameter Y on particle diameter with different packet porosities: 1) $\varepsilon = 0.48$; 2) 0.6. d_p, m.

Fig. 3. Steady-state temperature distribution in a packet consisting of 10 rows of particles (a — $\varepsilon = 0.48$; b — 0.6): 1) without allowance for phase heat exchange; 2-4) with allowance for phase heat exchange: 2) d_p = 0.1 mm; 3) 0.3; 4) 1 mm.

constant regardless of the time of contact with the surface and is equal to t_b. A temperature distribution typical of gas-convection models [3, 4] is formed in the bed.

Equations (7) and (8) make it possible to qualitatively evaluate the range of d_p in which the limiting models — an unblown packet for fine particles and gas-convection transfer for coarse particles — are valid. As boundaries we may take those values of the parameter Y at which the steady-state distribution of the temperature of the particles in a packet differs no more than 5% from the temperature distribution in the corresponding limiting models. Then the conditions of applicability of these models can be written in the form

$$Y > 9.5 \tag{9a}$$

for conventional packet models and

$$Y < 0.026 \tag{9b}$$

for models of gas-convection external heat exchange.

Figures 2-4 show the dependence of the parameter Y, the steady-state temperature distribution in the packet, and the complex K on the size of the fluidized particles. We took the following values for the parameters of the gas—air system under normal conditions: ρ_g = 1.293 kg/m^3; $\nu = 133 \cdot 10^{-7}$ m^2/sec; $\lambda_g = 24 \cdot 10^{-3}$ W/m·°K; ρ_p = 2500 kg/m^3; C_p = 1012 J/kg·°K. The results are shown for $\varepsilon = 0.48$ and $\varepsilon = 0.6$ in connection with the fact that, according to the data in [5], the porosity of the packet may be substantially greater than in the case of minimal fluidization.

It can be seen from Fig. 2 that the dimensionless parameter Y is a rapidly decreasing function of particle diameter. An increase in packet porosity, other conditions being equal, causes a reduction in Y. For the system parameters adopted in our calculations, conditions (9) change as follows: with a packet porosity $\varepsilon = 0.48$, the conventional packet model is acceptable if $d_p < 0.35$ mm, while gas-convection completely determines external heat exchange in a bed of particles with $d_p > 7$ mm; at $\varepsilon = 0.6$, conditions (9a) and (9b) take the forms $d_p < 0.25$ mm and $d_p > 3.5$ mm, respectively.

Figure 3 shows the steady-state temperature distribution in a 10-row packet. It can be seen from the figure that a profile with the main temperature gradient localized near the surface of the heat exchanger is formed when d_p increases. In contrast to our study, the

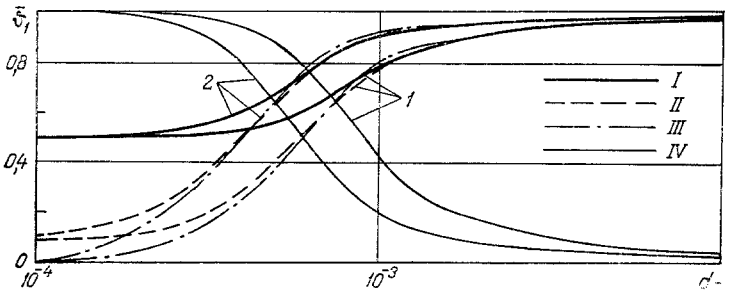

Fig. 4. Steady-state temperature of the first row in a packet and the parameter K in relation to particle size: 1) ε = 0.48; 2) 0.6; I) $\bar{\vartheta}_1^1$; II) $\bar{\vartheta}_1^{10}$; III) $\bar{\vartheta}_1^{\infty}$; IV) K. ϑ_1, °K.

analogous temperature distribution in [6] is explained exclusively by the thermal inertia of the particles, not having time to cool while the packet is near the wall.

Figure 4 shows the dependence on d_p of the parameter K and the steady-state temperature of the row of particles closest to the wall with N = 1, N = 10, and N → ∞. It can be seen that the value of $\bar{\vartheta}_1^N$ changes within a fairly broad range of particle diameters from a value typical of the packet model to the value used in gas-convection models $\bar{\vartheta}_1^N = 1$. Here, there is a rapid decrease in the time taken to establish a steady-state temperature distribution in the packet.

The coefficient of heat transfer between the packet and the surface is determined from the formula

$$\mathrm{Nu_e}(\tau) = \frac{\vartheta_1^N(\tau)}{y_p \varepsilon}. \tag{10}$$

It follows from (10) that the calculated value of the heat-transfer coefficient should depend on the size of the packet (the number of rows of particles N). In particular, using (5), for a single-row packet the following expression can be written for the dimensionless heat-transfer coefficient:

$$\mathrm{Nu_e}(\tau) = \frac{1}{y_p \varepsilon}\left[\frac{Y}{1+2Y}\exp\left(-\frac{\tau}{K\tau_0}\right) + \bar{\vartheta}_1^1\right]. \tag{11}$$

The mean value of the coefficient over the time of contact of the packet with the surface τ' is determined by the relation

$$\langle \mathrm{Nu_e} \rangle_{\tau'} = \frac{1}{y_p \varepsilon}\left[\frac{Y}{1+2Y}\frac{K\tau_0}{\tau'}\left(1-\exp\left(-\frac{\tau'}{K\tau_0}\right)\right) + \bar{\vartheta}_1^1\right]. \tag{12}$$

Let us see how Eqs. (11) and (12) change in relation to particle size and time of packet contact with the surface. For very small particles Nu* → 0, Y → ∞, so that

$$\mathrm{Nu_e}(\tau) \to \frac{1}{2\,y_p \varepsilon}\left[1+\exp\left(-\frac{\tau}{\tau_0}\right)\right],$$
$$\langle \mathrm{Nu_e} \rangle_{\tau'} \to \frac{1}{2\,y_p \varepsilon}\left[\frac{\tau_0}{\tau'}\left(1-\exp\left(-\frac{\tau'}{\tau_0}\right)\right) + 1\right]. \tag{13}$$

The effect of phase heat exchange in this case is negligibly small, and it can be assumed that no gas flows through the packet.

For very large particles Nu* → ∞, Y → 0,

$$\mathrm{Nu_e}(\tau) \to \frac{1}{y_p \varepsilon}, \quad \langle \mathrm{Nu_e} \rangle_{\tau'} \to \frac{1}{y_p \varepsilon}. \tag{14}$$

The temperature of coarse particles remains constant due to intensive phase heat exchange, and the coefficient of heat transfer between the packet and the surface does not depend on the contact time.

For very short contact times ($\tau' \to 0$), limiting values of Nu_e and $\langle Nu \rangle$ which are finite in accordance with [1-6] are determined by Eqs. (14), as for the case of coarse particles. In particular, for a dense bed, considering that the porosity of the row of particles closest to the wall $\varepsilon \approx 0.5$ [9] and $y_p = 1$, it is easy to obtain $Nu_e = 2$ from (14). This value agrees with the test data in [7]. Thus, the rate of heat transfer between the packet and surface at limitingly short contact times is determined mainly by the arrangement of the particles at the wall of the heat exchanger.

In the case of very long times of contact of the packet and surface, which are probable when there is poor mixing of the solid phase, the following limit relation may be obtained:

$$Nu_e = \langle Nu_e \rangle_{\tau'} = \frac{1}{y_p \varepsilon} \frac{1+Y}{1+2Y}. \tag{15}$$

Several conclusions can be drawn from the assumption made here regarding the role of phase heat exchange in the packet mechanism of external heat transfer and the results obtained on the basis of this model.

The proposed model subsumes the conventional model as a special case realized in the fluidization of fine particles. Another limiting case of the proposed model is an isothermal packet in the case of coarse particles, for which the main mechanism of external heat transfer is gas-convection transport. Heat transfer can be calculated for an intermediate range of particle sizes as well, when the temperature profile in the packet is different from the limiting cases.

The results of the calculations — temperature distribution, heat-transfer coefficient, time of establishment of steady-state temperature profile in the packet — are determined to a significant degree by a dimensionless parameter equal to the ratio of the heat flows due to conduction from the packet to the surface of the heat exchanger and due to phase heat exchange, i.e., from the core of the bed to the packet.

The modified packet model corresponds to a two-stage heat-transfer mechanism: the gas, the main heat carrier in beds of particles of any size, transfers heat from the core of the bed to particles in a packet as a result of phase heat exchange; the particles, being an intermediate heat carrier, transfer heat to the surface with which the packet is in contact by conduction through intervening gas layers. Here, the packet of particles can be likened to a movable system of ribs on the heat-exchanger wall.

In a bed of fine particles, the effective phase heat exchange is negligible, and a single-stage representation of the packet mechanism is quite suitable — here, the particles being regarded as sinks for heat accumulated in the core of the bed. In the case of coarse particles, the high-intensity phase heat exchange that occurs fully compensates for the loss of heat from particles near the surface. In this case, particles are excluded from the process of external heat exchange, and gas-convection transport is the only mechanism of heat transfer.

Thus, the proposed modified packet model can be applied to beds of particles of any sizes.

NOTATION

C, heat capacity; c_1, c_2, coefficients of equations of system (4); d_p, diameter of particles; K, dimensionless parameter; l_g, thickness of gas interlayer in model; t, temperature; U, gas velocity; y_p, dimensionless distance between centers of adjacent particles, expressed in terms of their diameters; Y, dimensionless parameter; α, coefficient of heat transfer between fluidized bed and surface; α^*, interphase heat transfer coefficient; ε, porosity; λ, thermal conductivity; ν, kinematic viscosity; ρ, density; τ, time; τ_0, time constant for a single-row unblown packet; τ', time of contact of packet with surface; ϑ_i^N, dimensionless temperature of the i-th row of particles of an N-row packet; $Ar = 9{,}81\, d_p^3(\rho_p/\rho_g - 1)/\nu^2$, $Nu_e = \alpha d_p/\lambda_e$, $Nu^* = \alpha^* d_p/\lambda_g$, $Pr = \nu C_g \rho_g/\lambda_g$, $Re = U d_p/\nu$. Indices: w, wall; b, core of bed; e, effective; g, gas; p, particles; $\bar{\vartheta}$, steady-state value; $\langle\ \rangle$, mean.

LITERATURE CITED

1. J. S. Botterill, Fluid-Bed Heat Transfer, Academic Press (1975).
2. O. M. Todes and O. B. Tsitovich, Equipment with a Fluidized Bed [in Russian], Khimiya, Leningrad (1981).
3. A. P. Baskakov (ed.), Heat- and Mass-Transfer Processes in a Fluidized Bed [in Russian], Metallurgiya, Moscow (1978).
4. V. A. Borodulya, V. L. Ganzha, and V. I. Kovenskii, Hydrodynamics and Heat Exchange in a Fluidized Bed under Pressure [in Russian], Nauka i Tekhnika, Minsk (1982).
5. K. E. Makhorin, V. S. Pikashov, and G. P. Kuchin, Heat Exchange in a High-Temperature Fluidized Bed [in Russian], Naukova Dumka, Kiev (1981).
6. A. P. Baskakov, High-Rate Nonoxidative Heating and Heat Treatment in a Fluidized Bed [in Russian], Metallurgiya, Moscow (1968).
7. N. V. Antonishin and V. V. Lushchikov, "Heat transfer in dispersed media," in: Investigation of Transport Processes in Dispersed Systems [in Russian], ITMO AN Belorussian SSR (A. V. Lykov Institute of Heat and Mass Transfer of the Belorussian Academy of Sciences), Minsk (1981), pp. 113-129.
8. L. L. Vasil'ev and S. A. Tanaeva, Thermophysical Properties of Porous Materials [in Russian], Nauka i Tekhnika, Minsk (1971).
9. M. É. Aérov and O. M. Todes, Hydraulic and Thermal Principles of the Operation of Units with Packed and Fluidized Beds [in Russian], Khimiya, Leningrad (1968).

EXPERIMENTAL DETERMINATION OF THE POROSITY FIELD IN A FLUIDIZED BED BY THE RADIOISOTOPE METHOD

N. N. Prokhorenko and S. A. Tikhomirov

UDC 66.096.5:537.2.24

We propose a method for constructing the concentration field of the solid phase in a disperse system which differs from conventional methods in that performing the measurements does not affect the hydrodynamics of the system.

The experimental method of constructing the concentration field of the solid phase or the porosity of a disperse system is based on the measurement of the spatial coordinates of a representative particle tagged with the isotope ^{60}Co [1]. It was shown in [1] that a coordinate can be measured to an accuracy of $\pm 11 \cdot 10^{-3}$ m in apparatus of diameter D = 0.25 m and height 0.75 m. The accuracy of the measurement of a coordinate can be increased by an order of magnitude by increasing the response speed of scintillation counters to 10^{-7}-10^{-8} sec with an efficiency no worse than 10%. With such scintillators the absolute velocity of a particle can be determined with a probable accuracy of $\pm 2 \cdot 10^{-2}$ m/sec.

The concentration field of the solid phase or the porosity is determined experimentally by using an empirical probability density distribution function, the histogram of the random vector with components x, y, z, $|x| \leqslant D/2$, $|y| \leqslant D/2$, $0 \leqslant z < \infty$.

In constructing a histogram it is necessary to solve three fundamental problems: 1) into what sized cells should the coordinate axes be divided; 2) how many measurements should be made of the random quantity, i.e., what should the sample size be; 3) what are the necessary conditions to ensure mutual independence, in the probabilistic sense, of the magnitudes of any two measurements.

A cell in which the porosity is measured should contain enough (N) granules to permit neglecting the statistical fluctuations of the porosity, the relative fraction of which is determined by the magnitude of $1/\sqrt{N}$ [2]. On the other hand, the size of a cell is fixed from below by the accuracy of the measurement of the coordinate of the tagged particle. In our case we chose a $2 \cdot 10^{-2}$ m cell.

P. P. Budnikov All-Union Scientific-Research Institute of Building Materials and Structures, Moscow. Translated from Inzhenerno-Fizicheskii Zhurnal, Vol. 47, No. 5, pp. 796-799, November, 1984. Original article submitted June 22, 1983.

 0022-0841/84/4705-1328$08.50